

**Interface phonons in InAs and AlAs quantum dot structures**

A. G. Milekhin,\* A. I. Toropov, A. K. Bakarov, and D. A. Tenne  
*Institute of Semiconductor Physics, 13 Lavrentiev Av., 630090, Novosibirsk, Russia*

G. Zanelatto and J. C. Galzerani  
*Departamento de Física, Universidade Federal de Sao Carlos, C.P. 676, Sao Carlos, SP, Brasil*

S. Schulze and D. R. T. Zahn  
*Institut für Physik, Technische Universität Chemnitz, D-09107 Chemnitz, Germany*  
 (Received 31 October 2003; revised manuscript received 20 April 2004; published 25 August 2004)

We present an experimental study of InAs/AlAs(GaAs) periodical structures with InAs and AlAs quantum dots by means of Raman spectroscopy. Experiments on the asymmetric GaAs/InAs/AlAs quantum dot structures allowed us to investigate the interface phonons localized in the vicinity of corrugated dot/matrix interface and planar interface between the matrix and wetting layer. The interface phonon frequencies in the quantum dot structures determined from the experiment are compared to those calculated in the framework of the dielectric continuum model. A good agreement is obtained, especially if the preferential shape of the quantum dots determined from transmission electron microscopy is taken into account.

DOI: 10.1103/PhysRevB.70.085314

PACS number(s): 68.65.Hb, 63.22.+m, 78.30.Fs

**I. INTRODUCTION**

It is well known that molecular beam epitaxy (MBE) of materials having a large lattice mismatch leads under certain conditions (Stranski-Krastanov growth mode) to spontaneous formation of dislocation-free small-size quantum dots (QDs).<sup>1</sup> A variety of materials (Ge/Si, (In, Ga, Al)Sb/GaAs, In(As, Sb)/InP, (Al, Ga)As/InAs) has been used for the formation of QD arrays.<sup>2-6</sup> Their optical and electronic properties promising for various device applications have become a subject of numerous investigations.<sup>1</sup>

Even though vibrational spectra of QD structures provide valuable information on structural properties of QDs such as size, shape, strain and atomic intermixing, the phonon properties of QD structures are much less investigated. Most of the published data related to phonons in QDs were obtained by Raman scattering experiments and refer mainly to Ge/Si<sup>7-9</sup> and InAs/GaAs QDs.<sup>4,10-12</sup> Pusep *et al.*<sup>4,10</sup> investigated the effect of topology on the interface (IF) modes localized near the edges of the dots in a single InAs QD layer embedded in GaAs. Recently, we reported a study of acoustic and optical phonons in structures with InAs QDs embedded in an AlAs matrix, as well as GaAs and AlAs nanosize islands (“antidots”) in an InAs matrix.<sup>3,9,13,14</sup>

In the present study we focus on the interface phonons in InAs/AlAs(GaAs) periodical structures with InAs and AlAs QDs. Raman scattering by IF phonons localized near QDs/matrix and wetting layer (WL)/matrix interfaces is observed. The frequency positions of the IF phonons obtained from Raman measurements are in good agreement with those calculated using the dielectric continuum model.

**II. EXPERIMENTAL DETAILS**

The nanostructures studied were grown by MBE in a Riber 32P system on (001)-oriented GaAs substrates utilizing

Stranski-Krastanov growth mode. Sample A, consisting of 50 periods of AlAs QDs embedded in InAs, was grown on a 1.5  $\mu\text{m}$  InAs buffer doped with silicon atoms ( $N_{\text{Si}}=2 \times 10^{18} \text{ cm}^{-3}$ ) at the substrate temperature of 420 °C. Each period contains an AlAs QD layer [(nominal thickness 2.4 monolayers (ML), 1 ML=0.283 nm)] and a 12-nm-thick InAs layer.

In order to distinguish between IF modes of the bottom, planar interface (WL/matrix) and those of the upper corrugated interface (QDs/matrix), InAs QD structures with asymmetric barriers were grown. Samples B and C are composed of ten periods of 3 ML InAs deposited on a 5 nm AlAs layer and overgrown by 35 nm of AlAs (sample B) or GaAs (sample C). In sample D, also containing ten periods, the 3 ML InAs layers were grown on a 5 nm GaAs layer and covered by 35 nm of AlAs. Delta doping of the GaAs and AlAs barriers was performed 2 nm below each InAs quantum dot layer in order to achieve a sheet carrier density of  $2 \times 10^{12} \text{ cm}^{-2}$ . Delta doping does not affect the phonon spectra of the QDs under investigation. It was made for irrelevant studies of electronic excitations in the spectral region far from the QD phonon frequencies. Sample B', which was used for transmission electron microscopy studies, is similar to sample B and was grown under the same conditions. Sample B' consists of ten 3 ML InAs QD layers separated by 25 nm AlAs spacer layer.

The substrate temperature was 500 °C during the growth of InAs QDs at an arsenic pressure of  $8 \times 10^{-6}$  Torr. After the deposition of the nominal amount of island material, the growth was interrupted for 12 s in the case of AlAs islands and 100 s for InAs QDs. The growth was monitored by reflection high energy electron diffraction (RHEED). According to RHEED data the transition from a two-dimensional to a three-dimensional growth mode (beginning of island formation) for all the samples occurs after the deposition of 1.8 monolayers of the island material. After the dot formation, the first 4 nm of AlAs (GaAs) spacers were grown at the

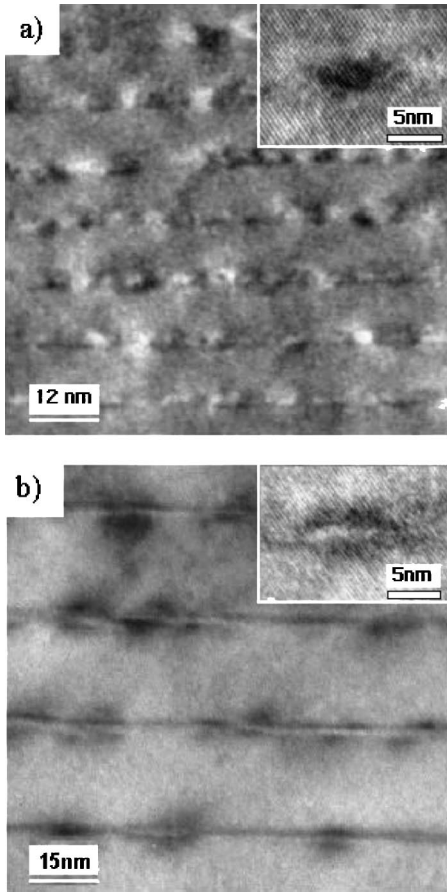


FIG. 1. Cross-sectional TEM images of samples with (a) AIAs (sample A) and (b) InAs QDs (sample B'). HRTEM images are shown in the insets.

same temperature, as QDs (500 °C). Then the temperature was increased up to 590 °C and the rest of the AIAs(GaAs) spacer was deposited. Two additional reference samples of GaAs/AIAs structures with the same layer sequences and thickness of AIAs and GaAs layers as those in samples C and D, but without InAs QD layers, were grown in using the same experimental conditions. These samples are denoted as C' and D', respectively.

The Raman spectra were recorded at  $T=20$  and 80 K using Dilor XY800 and Jobin Yvon T64000 triple spectrometers. The 514.5 and 647.1 nm lines of  $\text{Ar}^+$  and  $\text{Kr}^+$  lasers were used for excitation. The spectra were measured in backscattering geometries parallel to the growth axis and from the cleaved (110)-oriented edge. The scattering configurations employed were  $z(y,x)\bar{z}$ ,  $z(x,x)\bar{z}$  and  $y'(z,x')\bar{y}'$ ,  $y'(x',x')\bar{y}'$  with  $x,y,z,x',y'$  parallel to the [100], [010], [001],  $[1\bar{1}0]$  and [110] directions, respectively. For the backscattering experiments from a cleaved edge a microscope was employed to focus the light to a 1  $\mu\text{m}$  spot. The spectral resolution was 2  $\text{cm}^{-1}$  over the entire spectral range.

### III. RESULTS AND DISCUSSION

The structures under investigation were characterized by a high-resolution transmission electron microscopy (HRTEM).

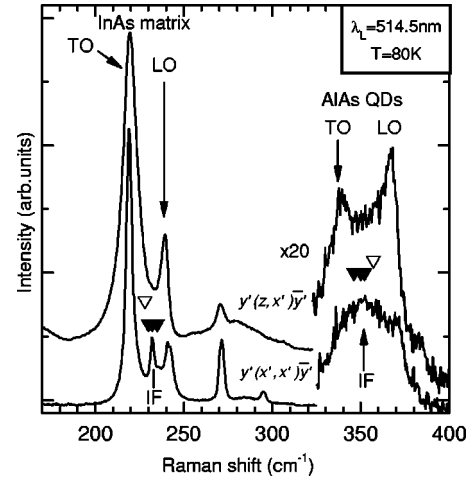


FIG. 2. Raman spectra of sample A at  $T=80$  K measured in the  $y'(x',x')\bar{y}'$  and  $y'(z,x')\bar{y}'$  scattering geometries excited by the 514.5 nm laser line. Closed and open triangles show the frequency positions of the IF phonons calculated for ellipsoidal and spherical QDs, respectively.

Cross-sectional TEM images shown in Fig. 1 reveal ellipsoidal and lens-like shape of AIAs (sample A) and InAs QDs (sample B'), respectively. The average sizes of AIAs QDs derived from HRTEM images are 4–5 nm base length and 2–4 nm height. InAs islands have larger base lengths ( $\sim 10$  nm) with a height of about 1.5 nm. It is worth mentioning that no wetting layer was observed for sample A, while the HRTEM images of InAs QD structures reveal the presence of an InAs wetting layer.

Figure 2 shows the Raman spectra of sample A measured in different scattering geometries, in which confined optical and/or IF phonons are observed. The spectra reveal strong peaks at 219 and 240  $\text{cm}^{-1}$  attributed to the TO and LO phonons of the InAs layers. Raman lines at 270 and 294  $\text{cm}^{-1}$  seen in both spectra are due to the TO and LO phonons of the GaAs substrate. Remarkable features at 339 and 367  $\text{cm}^{-1}$ , attributed respectively to the TO and LO phonons localized in the AIAs QDs, are shifted from their bulk positions due to the tensile strain in AIAs QDs.<sup>3</sup> It should be noted that the observed positions of the TO and LO phonons in AIAs dots in sample A differ from those reported in our earlier paper<sup>3</sup> for AIAs dots embedded in InAs (335 and 350  $\text{cm}^{-1}$ ). This difference can be due to the fact that the sample studied in Ref. 3 has a smaller nominal thickness of AIAs layers (2 ML), which is just above the threshold of QD formation (1.8 ML), while in sample A of the present work thicker AIAs layers were grown (2.4 ML). This resulted in larger dots (2–4 nm in height compared to 1.5–2 nm for the sample of Ref. 3). Therefore, there are a few possible reasons for a difference in the phonon frequencies. Larger dots can be less strained compared to smaller ones because of differences in size and shape (the dots of Ref. 3 apparently have the shape of truncated pyramids, while in sample A they seem to have ellipsoidal shapes), so the phonons are less shifted from the bulk frequency. Also, even though the confinement effect is considered to be small in AIAs dots (it was neglected in Ref. 3), still, it can cause an

additional downward shift of the phonon lines in the smaller dots of Ref. 3.

Raman spectra represented in Fig. 2 reveal additional features located at 232 and 351  $\text{cm}^{-1}$ , between the TO and LO phonon lines of AlAs QDs and InAs layers. These modes are attributed to InAs- and AlAs-like IF phonons originating from the QD/matrix interface. Their frequency positions were calculated in the frame of the dielectric continuum model.<sup>15</sup> In the calculation we supposed that AlAs QDs surrounded by InAs have a shape of an oblate ellipsoid with a ratio of the ellipsoid axes 2:1 corresponding to the value derived from HRTEM images. The results of the calculation are in good agreement with the experimental data. In the model, each IF mode is identified by two quantum numbers,  $l$  ( $l \geq 0$ ) and  $m$  ( $|m| \leq l$ ).<sup>15</sup> The IF modes with small quantum numbers are expected to contribute stronger to Raman scattering for QDs, since the modes with large  $l$  are strongly localized at the interface and couple weakly to charge carriers.<sup>15</sup> The calculated frequency positions of the first three InAs- and AlAs-like IF phonons (with quantum numbers  $l=1, m=0$  (230 and 352  $\text{cm}^{-1}$ ) and  $m=1$  (235 and 346  $\text{cm}^{-1}$ ); and  $l=2, m=0$  (232 and 350  $\text{cm}^{-1}$ ), respectively) are depicted in the Fig. 2 by closed triangles. According to Comas *et al.*,<sup>16</sup> only IF modes with  $l=\text{even}$  integer and  $m=0$  are allowed in Raman scattering. Therefore, the major contribution to the IF lines observed in the Raman spectra at 232 and 350  $\text{cm}^{-1}$  is most likely due to the IF modes with  $l=2, m=0$  (the middle closed triangles in Fig. 2). For comparison, the frequency positions of the IF phonons with quantum number  $l=1$  calculated for the structure with spherical QDs are shown by open triangles. One can see that the calculations for the ellipsoidal QDs correspond much better to the observed IF line positions. It is worth mentioning that due to the high symmetry of these QDs and the apparent absence of the wetting layers only one type of IF mode exists in the frequency ranges of QD and matrix materials, in contrast to the InAs QDs embedded in AlAs. The latter have two types of IF modes corresponding to the planar WL/matrix interface and corrugated interface between the QDs and the matrix.

Figure 3 shows the Raman spectra of samples B, C, and D with InAs QDs measured in the  $z(x,x)\bar{z}$  and  $z(y,x)\bar{z}$  scattering geometries in the spectral range of optical phonons in InAs and GaAs (Fig. 3(a)) and AlAs (Fig. 3(b)). Raman spectra of samples C' and D' (GaAs/AlAs structures without InAs QDs) are also presented for comparison. (We used the 647.1 nm laser line for samples B, C, and D since it is close to resonance with electronic transitions in InAs QDs embedded in AlAs. Spectra measured at 514.5 nm show weaker signals of the IF modes.) In the spectral region of InAs optical phonons only the Raman spectra of sample B contain a broad asymmetric feature of significant intensity in the range of 230–260  $\text{cm}^{-1}$  with a maximum at 256  $\text{cm}^{-1}$ . This feature is similar to that observed earlier in InAs/AlAs QD structures<sup>13,14</sup> and is attributed to the confined LO phonons of InAs QDs. Asymmetric line shape of the feature is explained by a contribution in the Raman signal of confined phonons with higher quantum numbers and/or IF phonons in InAs QDs. Raman scattering by the optical phonons confined in InAs QDs embedded in AlAs (sample

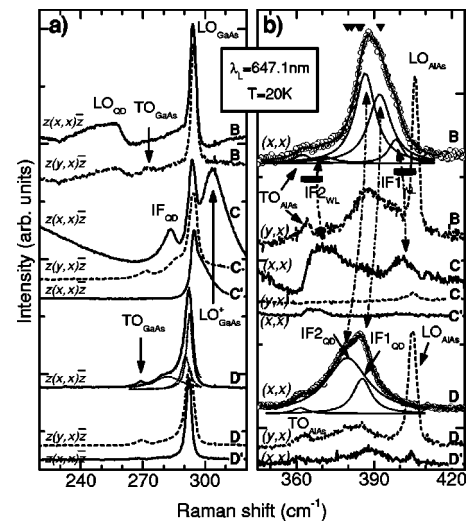


FIG. 3. Raman spectra of samples B, C, and D at  $T=20$  K measured with the 647.1 nm laser line in the  $z(x,x)\bar{z}$  and  $z(y,x)\bar{z}$  (dashed lines) scattering geometries in the spectral regions of GaAs, InAs (a) and AlAs (b). Raman spectra of samples C' and D' measured in the  $z(x,x)\bar{x}$  scattering geometries are shown for comparison. For samples B and D, the experimental spectra are shown by open circles, and thin solid lines represent the results of fitting by Lorentzian curves. Closed triangles show the calculated frequency positions of the IF phonons for QDs with the shape of oblate capsules. Horizontal bars show the calculated positions of interface phonon bands for planar interfaces in AlAs/InAs superlattices. Dashed-dotted lines are guides to the eye.

B) is enhanced due to the proximity of the excitation energy (1.92 eV) to the electronic transitions in InAs QDs in AlAs matrix (about 1.7–1.8 eV, according to photoluminescence data<sup>14,17</sup>). In samples C and D the band-gap energy of InAs QDs is expected to be significantly lower, since the QDs have lower barriers of GaAs at one side. Therefore, the excitation laser energy is far from resonance with electronic transitions in these samples. This explains the absence of noticeable Raman signal from InAs phonons in samples C and D.

In the GaAs frequency region, the spectra of sample B contain the lines from the GaAs substrate only, since this sample has no GaAs in the QD structure. Samples C and D have the corrugated InAs QD/GaAs and planar WL/GaAs interfaces, respectively, as well as GaAs/AlAs planar interfaces. In sample C, which has the an interface between QDs and GaAs, the spectrum contains a relatively intensive line at 283  $\text{cm}^{-1}$  (Fig. 3(a)), which is attributed to GaAs-like IF phonons from the corrugated InAs QDs/GaAs interface. The contribution of IF modes of GaAs/AlAs interface is expected at about the same frequency position in the middle between the LO and TO phonons of GaAs. A feature at 304  $\text{cm}^{-1}$  is a high frequency plasmon-phonon line in a delta-doped GaAs barrier. A low frequency plasmon-phonon line is also observed near 200  $\text{cm}^{-1}$  (not shown in the figure). In sample D we observed an asymmetric shoulder on the low frequency side of the GaAs LO phonon peak, which can be attributed to the IF mode of planar GaAs/WL interface, and a weak feature in the middle between the LO and TO

phonons, at about  $280\text{ cm}^{-1}$  (see Fig. 3(a), thin dotted lines show the results of fitting by Lorentzian curves). The latter can be due to the contribution of the IF modes from GaAs/AIAs interface. This line is much weaker compared to the line at  $283\text{ cm}^{-1}$  observed in sample C.

In the AIAs spectral region (Fig. 3(b)) the spectra of samples B, C, and D, (as well as C' and D', not shown) measured in the  $z(y,x)\bar{z}$  scattering geometry reveal features at  $363$  and  $405\text{ cm}^{-1}$  corresponding to the bulk-like TO and LO phonons of AIAs layers. The Raman spectrum of sample B measured in the  $z(x,x)\bar{z}$  scattering geometry shows a broad asymmetrical feature located between the frequency positions of the AIAs TO and LO phonons. The position and line shape of this feature can be explained by two effects. First, AIAs-like IF phonons at the corrugated InAs QDs/AIAs matrix interface contribute to the Raman scattering at a frequency position located approximately in the middle between the TO and LO phonons of AIAs. Second, the observed asymmetry of the broad line can be due to Raman scattering by AIAs-like IF phonons from the bottom WL/matrix interface. Since the thickness of AIAs layers exceeds significantly that of the InAs WL ( $\sim 0.6\text{ nm}$ ) the frequency positions of the IF phonons at the planar WL/matrix interfaces are expected to be close to the TO and LO phonons in AIAs.<sup>18,19</sup>

In order to distinguish between these contributions let us consider the Raman spectra of samples C and D. Each of these samples has only one type of InAs/AIAs interface: planar WL/matrix interface for sample C, and corrugated QD/matrix interface for sample D, while the second interface for these samples in InAs/GaAs. Therefore, the AIAs-like IF phonons originating from InAs QDs/AIAs matrix or InAs WL/AIAs matrix interfaces are alternatively excluded for samples C and D, respectively. The Raman spectrum of sample C contains no features in the middle between the frequencies of AIAs TO and LO phonons. Instead, two lines appear in the spectra, centered near  $370$  and  $400\text{ cm}^{-1}$ , which are assigned to the two bands of AIAs-like IF phonons at the planar interface between InAs WL and AIAs matrix. These modes are labeled as  $\text{IF1}_{\text{WL}}$  and  $\text{IF2}_{\text{WL}}$ . As mentioned above, a relatively strong line attributed to GaAs-like IF phonons from the corrugated InAs QDs/GaAs interface is present in the spectrum of sample C at  $283\text{ cm}^{-1}$  (Fig. 3(a)). It should be noted that in planar superlattices one of the IF bands in AIAs region is Raman active while the other is forbidden because of the symmetry with respect to the central plane parallel to of the superlattice layers.<sup>19</sup> In QD structures this symmetry is broken and both IF bands,  $\text{IF1}_{\text{WL}}$  and  $\text{IF2}_{\text{WL}}$ , are observed in the Raman spectra.

As expected, no features related to IF phonons at the WL/AIAs matrix interfaces are observed in the Raman spectra of sample D. However, an asymmetric doublet-like feature centered at  $382\text{ cm}^{-1}$  appears, which is attributed to the IF phonons of the corrugated InAs QDs/AIAs matrix interface. The splitting of the feature cannot be explained assuming a spherical shape of InAs QDs and indicates a lower symmetry of the QDs. Frequency positions of the modes are determined from the best fitting of the Raman spectrum measured in the  $z(x,x)\bar{z}$  scattering geometry by two Lorentzian curves centered at  $379$  and  $385\text{ cm}^{-1}$ , labeled as  $\text{IF1}_{\text{QD}}$  and  $\text{IF2}_{\text{QD}}$ , respectively.

A similar fitting procedure was performed for the Raman spectrum of sample B, which can be best fitted using four Lorentzian curves. They are referred to IF phonons from the corrugated InAs QD/AIAs ( $392$  and  $386\text{ cm}^{-1}$ ) and the planar InAs WL/AIAs interface ( $370$  and  $398.5\text{ cm}^{-1}$ ). The positions of the latter two lines are close to those of IF modes from planar interfaces observed in sample C. The IF modes of the corrugated QD/AIAs interface are similar to the “doublet” observed in sample D. The difference in frequencies of these modes in samples C and D can be due to the fact that in these samples the InAs dots were grown on different surfaces (AIAs in sample B and GaAs in sample D). Therefore the dots can have some differences in size and morphology. Another factor could be a possible contribution of the modes from GaAs/AIAs interfaces in sample D. This contribution is expected to be weak, based on the data of sample D', as discussed below, but it can slightly affect the position of the observed lines in sample D, while there are no GaAs/AIAs interfaces in sample B.

We calculated the IF phonon frequencies using the dielectric continuum model of Knipp and Reinecke,<sup>15</sup> assuming that InAs QDs have a shape of oblate capsules. According to the model, a set of IF modes identified by two quantum numbers,  $l$  ( $l \geq 0$ ) and  $m$  exists in capsule-like QDs. The calculated frequencies of the first 5 IF modes ( $l \leq 2, m = 0, 1$ ) are presented in Fig. 3 by triangles. As can be seen from Fig. 3, a good agreement between the calculated and experimental IF phonon frequencies is obtained for sample B. According to the calculation, the first IF mode (likely the most intensive one) is relatively separated from the others, which lie in a narrow frequency interval. This can give rise to asymmetric doublet-like feature observed in the spectra. The horizontal bars in Fig. 3(b) indicate the positions of interface phonon bands calculated using the dielectric continuum model<sup>18</sup> for planar AIAs/InAs superlattices with large ratio of thicknesses of AIAs and InAs layers, as in sample B. The calculated positions of the IF bands reveal reasonable agreement with the experimental data.

Theoretical studies of phonon modes in superlattices<sup>20</sup> and quantum dots<sup>21,22</sup> showed that more accurate description of phonons in low-dimensional systems has to take into account both electrostatic and mechanical boundary conditions. Such an approach describes the phonon modes as a mixture of confined and interface parts. However, phonon confinement effects are important for two-dimensional structures with ultrathin layers or very small quantum dots. Here we consider the IF modes at the boundaries of rather thick AIAs layers (InAs layers in sample A), and confinement effects are less significant. Therefore the dielectric continuum model of Knipp and Reinecke<sup>15</sup> provides a good description of the interface modes in our structures.

It should be noted that Zanelatto *et al.*<sup>10</sup> studied GaAs-like interface phonons in uncapped and capped InAs QD's in GaAs matrix and observed similar IF phonon lines in both cases. This led Zanelatto *et al.* to the conclusion that the bottom and top interfaces of their samples are likely similar, i.e., there is no planar WL/matrix interface due to In segregation. This is apparently not the case in our InAs/AIAs QD samples.

In the QD structures C and D IF phonons originating from GaAs/AIAs interface can also contribute to the Raman spec-

tra. To analyze the possible contribution of these interfaces we have studied samples C' and D', having the same GaAs/AlAs interfaces as samples C and D, but no InAs QD layers. Indeed, Raman spectra of samples C' and D' measured in AlAs spectral range in the  $z(x,x)\bar{z}$  scattering geometry contain the lines of IF phonons originating from the GaAs/AlAs interface. Their frequency positions and those of IF phonons from the InAs WL/AlAs interface lie in the same spectral regions, thus complicating identification of the modes. However, intensities of the IF phonon lines originating from the GaAs/AlAs interfaces are significantly smaller compared to those from InAs/AlAs interfaces. (See Fig. 3(b)); all the spectra are normalized by the intensity of the LO phonon of GaAs substrate.) The reason for this is as follows. The laser line used for excitation (1.92 eV) is significantly closer to the electronic transitions in InAs QDs and wetting layers (which are in the range 1.7–1.9 eV<sup>14,17</sup>), compared to those of GaAs. Therefore, the contribution to the Raman spectra from the IF phonons localized near InAs QDs and WL's is much stronger than the signal from the phonons of GaAs/AlAs interfaces. Moreover, no phonon lines related to the GaAs/AlAs interface can be seen in Raman spectra of samples C' and D' in the GaAs spectral region while a strong feature between LO and TO phonon frequencies is observed in the Raman spectrum of sample C, which is attributed to the IF modes at the interface between InAs QDs and GaAs capping layer. Therefore, we suppose that the IF

phonons from the GaAs/AlAs interface play no significant role in the identification of the observed modes.

#### IV. CONCLUSION

In summary, we performed an experimental Raman study of the vibrational spectra of multilayer InAs/AlAs(GaAs) structures with ensembles of InAs and AlAs QDs. TO and LO phonons confined in the QDs and IF phonons localized in the vicinity of QD/matrix and wetting layer/matrix interfaces were observed. Raman spectra measured in the asymmetric GaAs/InAs/AlAs QD structures allowed one to distinguish between the contributions of interface phonons at the planar WL/matrix interface and the corrugated QD/matrix interface. The positions of IF phonons in the QD structures observed in the experiment agree well with those calculated within the dielectric continuum model. A potential sensitivity of Raman spectroscopy to the preferential shape of QDs was demonstrated.

#### ACKNOWLEDGMENTS

This work was supported in part by the Volkswagen Foundation (Project No. I/76837), IN-TAS (Grant No. YS-2001/2-12/1B/D), FAPESP and the Russian Foundation for Basic Research (Grant No. 01-02-16969). We are thankful to Gisela Baumann for a sample preparation for the HRTEM experiments.

\*Electronic address: milekhin@thermo.isp.nsc.ru

- <sup>1</sup>D. Bimberg, M. Grundmann, and N. N. Ledentsov, *Quantum Dot Heterostructures* (Wiley, New York, 1999).
- <sup>2</sup>J. Groenen, R. Carles, S. Christiansen, M. Albrecht, W. Dorsch, H. P. Strunk, H. Wawra, and G. Wagner, *Appl. Phys. Lett.* **71**, 3856 (1997); **71**, 56 (1997).
- <sup>3</sup>D. A. Tenne, V. A. Haisler, A. I. Toropov, A. K. Bakarov, A. K. Gutakovskiy, D. R. T. Zahn, and A. P. Shebanin, *Phys. Rev. B* **61**, 13 785 (2000).
- <sup>4</sup>Yu. A. Pusep, G. Zanelatto, S. W. da Silva, J. C. Galzerani, P. P. Gonzalez-Borrero, A. I. Toropov, and P. Basmaji, *Phys. Rev. B* **58**, R1770 (1998).
- <sup>5</sup>G. Armelles, T. Utzmeier, P. A. Postigo, F. Briones, J. C. Ferrer, P. Peiro, and A. Cornet, *J. Appl. Phys.* **81**, 6339 (1997).
- <sup>6</sup>J. Groenen, A. Mlayah, R. Carles, A. Ponchet, A. Le Corre, and S. Salaün, *Appl. Phys. Lett.* **69**, 943 (1996).
- <sup>7</sup>A. Milekhin, A. I. Nikiforov, O. P. Pchelyakov, S. Schulze, and D. R. T. Zahn, *Physica E (Amsterdam)* **13**, 982 (2002).
- <sup>8</sup>A. G. Milekhin, A. I. Nikiforov, M. Ladanov, O. P. Pchelyakov, D. A. Tenne, S. Schulze, and D. R. T. Zahn, *Mater. Res. Soc. Symp. Proc.* **737**, E13.7.1 (2003).
- <sup>9</sup>A. Milekhin, D. A. Tenne, and D. R. T. Zahn, in *Quantum Dots and Nanowires*, edited by S. Bandyopadhyay and H. S. Nalwa (American Scientific, 2003), p. 375.
- <sup>10</sup>G. Zanelatto, Yu. A. Pusep, N. T. Moshegov, A. I. Toropov, P. Basmaji, and J. C. Galzerani, *J. Appl. Phys.* **86**, 4387 (1999).

- <sup>11</sup>L. Artus, R. Cusco, S. Hernandez, A. Patane, A. Polimeni, M. Henini, and L. Eaves, *Appl. Phys. Lett.* **77**, 3556 (2000).
- <sup>12</sup>J. Ibanez, A. Patane, M. Henini, L. Eaves, S. Hernandez, R. Cusco, L. Artus, Yu. Musikhin, and P. N. Brounkov, *Appl. Phys. Lett.* **83**, 3069 (2003).
- <sup>13</sup>D. A. Tenne, V. A. Haisler, A. K. Bakarov, A. I. Toropov, A. K. Gutakovskiy, A. P. Shebanin, and D. R. T. Zahn, *Phys. Status Solidi B* **224**, 25 (2001).
- <sup>14</sup>D. A. Tenne, A. K. Bakarov, A. I. Toropov, and D. R. T. Zahn, *Physica E (Amsterdam)* **13**, 199 (2002).
- <sup>15</sup>P. A. Knipp and T. L. Reinecke, *Phys. Rev. B* **46**, 10 310 (1992).
- <sup>16</sup>F. Comas, C. Trallero-Giner, N. Studart, and G. E. Marques, *Phys. Rev. B* **65**, 073303 (2002).
- <sup>17</sup>T. S. Shamirzaev, A. M. Gilinsky, A. K. Bakarov, A. I. Toropov, D. A. Tenne, K. S. Zhuravlev, C. von Borczyskowski, and D. R. T. Zahn, *JETP Lett.* **77**, 389 (2003); *Physica E (Amsterdam)* **20**, 282 (2004).
- <sup>18</sup>R. E. Camley and D. L. Mills, *Phys. Rev. B* **29**, 1695 (1984).
- <sup>19</sup>A. K. Sood, J. Menendez, M. Cardona, and K. Ploog, *Phys. Rev. Lett.* **54**, 2115 (1985).
- <sup>20</sup>A. J. Shields, M. P. Chamberlain, M. Cardona, and K. Eberl, *Phys. Rev. B* **51**, 17 728 (1995).
- <sup>21</sup>E. Roca, C. Trallero-Giner, and M. Cardona, *Phys. Rev. B* **49**, 13 704 (1994).
- <sup>22</sup>M. P. Chamberlain, C. Trallero-Giner, and M. Cardona, *Phys. Rev. B* **51**, 1680 (1995).